Regional-scale convection patterns during strong and weak phases of the Saharan heat low

Christophe Lavaysse, Cyrille Flamant, Serge Janicot

ATMOSPHERIC SCIENCE LETTERS
Atmos. Sci. Let. **11**: 255–264 (2010)
Published online 16 August 2010 in Wiley Online Library
(wileyonlinelibrary.com) **DOI:** 10.1002/asl.284

RMetS
Royal Meteorological Society

Regional-scale convection patterns during strong and weak phases of the Saharan heat low

C. Lavaysse,[1,2]* C. Flamant[2] and S. Janicot[3]

[1] *Laboratoire d'Etude des Transferts en Hydrologie et Environnement, CNRS and Université Joseph Fourrier, Grenoble, France*
[2] *Laboratoire Atmosphère, Milieux, Observations Spatiales, CNRS and Université Pierre et Marie Curie, Paris, France*
[3] *Laboratoire d'Océanographie et du Climat: Expérimentation et Approches Numériques, IRD and Université Pierre et Marie Curie, Paris, France*

**Correspondence to:*
C. Lavaysse, Laboratoire d'Etude des Transferts en Hydrologie et Environnement, BP53 Domaine Universitaire, Grenoble, France.
E-mail:
christophe.lavaysse@gmail.com

Abstract

The West African heat low, which is defined as a thermal depression generally below 700 hPa over West Africa, is stationary over the Sahara during the summer season and is often referred to as the Saharan heat low (SHL). This SHL displays synoptic and intra-seasonal pulsations of its intensity on time scales under 60 days.

In this study, we analyse the regional-scale pattern of low troposphere dynamics and convective activity associated with weak and strong phases of the SHL during the summer, using 18 years (1984–2001) of concomitant European Centre for Medium-range Weather Forecasts re-analysis data and satellite observations of brightness temperature provided by the European Union-funded Cloud Archive User Service. Strong SHL phases, defined by an increase of low-level atmospheric thickness, are accompanied by (1) a positive anomaly of temperature in the low layers, (2) a strengthening of the monsoon flow, (3) both a negative anomaly of the divergence flux and an enhancement of the moisture advection over the central Sahel, (4) an intensification of the African easterly jet and (5) enhanced upward vertical motions located south of the inter-tropical discontinuity (ITD). These conditions appear to be favourable for the occurrence of convection over the central Sahel. The strongest, most widespread convective activity over the central and eastern Sahel occurs on the day when the SHL intensity is the strongest. In contrast, a significant decrease of the convective activity was detected over Senegal and to the West of the Jos Plateau.

Opposite patterns are found during weak SHL phases, with a negative anomaly of convection over the central and eastern Sahel connected with anomalous subsidence south of the ITD and a negative moisture advection anomaly. Conversely, convection is seen to be enhanced along the Atlantic coast and particularly over Senegal.

Received: 29 September 2009
Revised: 19 March 2010
Accepted: 2 June 2010

Keywords: **West African Monsoon; convective activity; precipitation; synoptic circulation; AMMA**

1. Introduction

Over West Africa, the intensity and the direction of the winds at low levels, such as the monsoon and the Harmattan winds, are closely linked to surface pressure gradients. The inter-tropical discontinuity (ITD) marks the surface position of the interface between the cool, moist south-westerly monsoon flow and the hot, dry north-easterly Harmattan flow. The ITD is generally characterized by strong convergence and low pressures at low levels.

Furthermore, over the West African continent, an area of high surface temperatures and low surface pressures (i.e. a heat low) exists throughout the year and is located where insolation is high and evaporation is low (Lavaysse *et al*., 2009 (LA09)). The surface pressure and the dilatation of the atmosphere at low-level generated by an increase of the temperature are commonly used to define the state (or intensity) of the heat low, which is strongest when it is associated with a large temperature-induced low levels atmospheric depth. In the summer, the West African heat low is generally positioned over the Sahara and is often referred to as the Saharan heat low (SHL). During this period, the SHL is considered to be a major dynamical element of the West African Monsoon system (see LA09 and references therein).

Using an idealized model, Ràcz and Smith (1999) have illustrated the impact of the Australian heat low on atmospheric circulation over the idealized Australian continent. The authors have shown that a strong cyclonic circulation develops in the low troposphere around the heat low centre. They point out that the strength of the low-level circulation has a large diurnal cycle with the strongest circulation in the early hours of the morning. Spengler and Smith (2008), using another set of idealized simulations, have illustrated that the wind speed in the low troposphere, associated with this cyclonic circulation, increases each day. This evolution is consistent with the gradual growth of maximum temperature in the mixed layer along 6 days of simulations. Over West Africa, the cyclonic

circulation associated with the SHL contributes to increase both the south-westerly monsoon flow along its eastern flank and the north-easterly Harmattan flow along the western flank, especially when the low-level temperatures are high and the induced cyclonic circulation is stronger. Knippertz (2008) and Parker *et al*. (2005) have suggested that such a circulation is likely to enhance the probability of moist convection and cloud cover poleward of the main rainy zone to the East of the SHL. However, the suggestion made by these authors is based only on a few cases and no attempt has been made to date to assess the relevance of this hypothesis using a more extensive data set. Furthermore, two recent studies have highlighted the fact that the SHL exhibits intensity pulsations at the intra-seasonal scale. Such fluctuations would arguably have an impact on low-level dynamics (especially the monsoon flow intensity) and, in turn, on moisture advection over the Sahel. Parker *et al*. (2005) showed that the diurnal cycle of winds (dominated by nocturnal advection) in Niamey (Niger) was correlated at synoptic and intra-seasonal time scales with the temperature to the north. Couvreux *et al*. (2009) have discussed the impact of SHL intensity fluctuations on the northward monsoon surges during a few days in spring (before the monsoon onset) and show that such surges occur after strong SHL episodes. Using a more extensive data set (18 years of European Centre for Medium-range Weather Forecasts (ECMWF) re-analyses), Lavaysse *et al*. (2010) have detailed the complex interactions that exist between the SHL intensity pulsations at intra-seasonal time scale during the summer with the low-level and mid-level dynamics on the regional scale. In particular, they analyse the impact of African easterly waves and of mid-latitude circulations on the SHL intensity pulsations at 3–10 days and 10–30 days, respectively.

To date, the relationship between the SHL intensity and the convection patterns over West Africa has not been investigated during the summer season. To the best of the authors' knowledge, this study is the first attempt to do so. Using two independent, extensive data sets (18 years of concomitant ECMWF re-analyses and satellite data), this article aims at analysing the large-scale circulation and convection patterns over West Africa during extreme SHL intensity cases. Large-scale conditions associated with both very strong and very weak composited SHL events during the summer are investigated.

This article is organized as follows. The data set and the method used to detect the specific components of the West African monsoon are presented in Sections 2 and 3. The SHL intensity classification method is explained in Section 4 and the composite method is detailed in Section 5. The impact of the SHL intensity fluctuations on the low-level circulation, the vertical structure of the troposphere and convective activity is detailed in Sections 6, 7 and 8, respectively.

2. Data set

In this study, 18 years of concomitant ECMWF re-analysis and brightness temperature observations provided by the European Union-funded Cloud Archive User Service (CLAUS, http://badc.nerc.ac.uk/data/claus/) are used (between 1984 and 2001). The period selected was based on data availability (1984–2004 for CLAUS and 1967–2001 for ECMWF) and the fact that the 1979–2001 period is generally regarded as the more reliable part of the data set for climatological analysis ((Kallberg *et al*., 2005)).

The model variables are available on 23 pressure levels between 1000 and 1 hPa, with a horizontal resolution of $1.125° \times 1.125°$. The following fields have been used in this study: the three components of the wind as well as temperature and water vapour mixing ratio. As explained later, only data at 0600 UTC are used.

The brightness temperature obtained from the CLAUS archive is based on the level B3 10 μm radiances from operational meteorological satellites participating in the International Satellite Cloud Climatology Programme (ISCCP, Brest *et al*., 1997). The CLAUS project maintains a long time series of three-hourly global images of the Earth in the thermal infra-red images window. The infra-red brightness temperature fields from the CLAUS archive have been interpolated onto a regular latitude–longitude grid at a spatial resolution of $0.5° \times 0.5°$. Brightness temperatures below 230 K (which are generally associated with the top of deep convective clouds) were used to build a climatology of the frequency of occurrence of deep convection over the area of interest, as in Fu *et al*. (1990).

3. Method

LA09 have used an empirical orthogonal function analysis to establish the time period when the SHL is stationary over the Sahara during the summer (on average between 20 June, ±9 days, and 17 September, ±7 days, over a period of 23 years). This period shows low inter-annual variability and occurs during the summer season over West Africa. It is associated with a great part of the cumulative rainfall during the year over the Sahel. In this article, the summer season refers to this period, when the large-scale dynamic components of the Monsoon system are well established.

3.1. Daily ITD detection

On horizontal maps, the position of the ITD is determined by meteorologists from surface dew-point temperature and/or wind direction measurements (Buckle, 1996; Lafore *et al*., 2007). Difficulties in comparing different analyses of the ITD, as reported in the literature, are related to the choice of dynamic (wind-based) *versus* thermodynamic criteria and the diurnal

variations. In the framework of the African Monsoon Multidisciplinary Analysis (AMMA, Redelsperger *et al*., 2006), the forecasters used three criteria to provide daily forecasts of the ITD position at 0600 UTC to the special observation period scientists: near surface convergence, a dew-point temperature of 15 °C and pressure that should exhibit a local minimum at the ITD (Lafore *et al*., 2007).

In this article, the position of the ITD is identified from the convergence criterion above applied to the 925 hPa wind field of the ECMWF analyses.

3.2. Daily SHL detection

We detect the SHL using the method proposed by LA09, i.e. using a criterion based on the dilatation of the lower atmosphere generated by an increase of the temperature at low level as a result of surface heating to identify the presence of the SHL. To do so, we estimate the low-level atmospheric thickness between two pressure levels of the re-analyses. The upper-level boundary is chosen as 700 hPa (around 3500 m above mean sea level on average over West Africa). This prevents spurious detection of geopotential anomalies in the upper atmosphere due to mid-level circulations as explained in LA09. The lower boundary is selected as 925 hPa. We use ECMWF fields at 0600 UTC only to avoid turbulent mixing effects in the planetary boundary layer and to obtain the strongest geostrophic low-level winds over West Africa.

The SHL detection algorithm runs in three steps on a given day of a given year: (1) the atmospheric thickness is calculated between 925 and 700 hPa from the 0600 UTC geopotential field; (2) a cumulative probability distribution function of the low-level atmospheric thickness is computed on all of the 1702 grid points of the domain extending over West Africa and adjacent Tropical Atlantic, i.e. between 20 °W and 30 °E and between 0°N and 40°N; and (3) the SHL is defined as the area where the low-level atmospheric thickness exceeds a threshold defined as 90% of the thickness cumulative probability distribution function (i.e. the highest 10% values of thickness). A relative (i.e. daily) threshold rather than an absolute threshold is used because, on a given day, the SHL is defined as a depression relative to its environment.

3.3. Moisture budget in the low troposphere

To estimate the impact of the SHL in the low troposphere, we used different components of the moisture budget presented here.

The moisture advection is computed for each day (at 0600 UTC) and each level independently using $\overrightarrow{V} \cdot \nabla q$, where $\overrightarrow{V}$ is the horizontal wind vector and q is the water vapour mixing ratio issued by the ECMWF re-analysis. Then, to analyse the moisture advection in the low troposphere and especially in the monsoon layer, the advection term has been integrated between 925 and 850 hPa.

Using the same wind and moisture fields, we estimate the low troposphere water vapour flux divergence following $\nabla(\overrightarrow{V} \cdot q)$. This divergence term is then also integrated between 925 and 850 hPa. Note that following Lenters and Cook (1995), this divergence flux can be decomposed in moisture advection (presented above) and moisture divergence.

4. SHL intensity classification

In the following, the low-level atmospheric thickness is used as a proxy for the intensity of the SHL, thick layer values being indicative of a strong dilatation of the lower atmosphere in response to an increase of temperature at low-level and hence of a strong SHL.

Here, we investigate intensity fluctuations of the SHL over the Sahara during the 20 June to 17 September period. The most significant time scales of SHL intra-seasonal variability during this period were obtained via a wavelet analysis, using a Morlet mother wave (Torrence and Compo, 1998). This analysis showed that the most significant signal was obtained for time periods under 30 days (not shown). To focus on these periods and to avoid contamination by variability at the seasonal scale, the time series of daily SHL thickness was filtered using a high-pass Kaiser filter, with a cut-off frequency at 60 days. This cut-off frequency is the same as the one chosen by Sultan *et al*. (2003) to analyse the intra-seasonal variability of the mean daily rainfall over the Sahel. Note that the number of classes selected here is arbitrary.

On the basis of the climatological summer location of the West African heat low over the Sahara, we select a domain where the occurrence probability of the SHL cumulated over the 18 years exceeds 75%. This core area extends from 10 °W to 7 °E and from 19°N to 27°N. Days when the centre of the SHL is not located in this area are discarded thereafter. As in LA09, the centre of the SHL is defined as the average of the positions of the grid points at which the depth of the SHL exceeds the threshold value, weighted by the SHL depth at this point. A total of 1540 days were retained. Then, daily low-level atmospheric thickness values have been aggregated in 20 classes containing 77 cases. Class # 20 contains the largest thicknesses and class # 1 contains the least thicknesses cases of SHL encountered during the 18-year period.

Figure 1 shows that the increase of the SHL intensity (as defined from the atmospheric thickness values, see above) is associated with a decrease of the integrated column pressure (1000 hPa geopotential height) in the region of the SHL, to the north of the ITD. It is worth noting that there is no latitudinal displacement of the mean position of the lowest 1000 hPa geopotential height values, which is seen as a function of the SHL intensity. In each SHL class, the centre of lowest pressure is around 22°N. The position of the centre of the SHL, as well as its intensity, has a significant impact on the speed and direction of

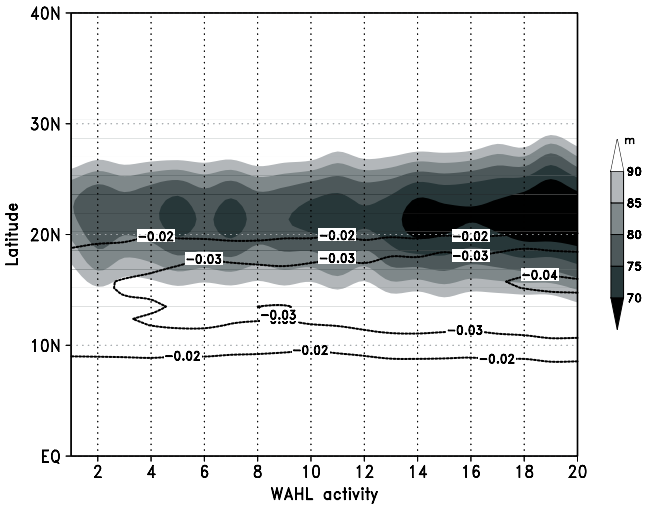

Figure 1. Mean 1000 hPa geopotential height (shaded), averaged between 15 °W and 10 °E, classified as a function of SHL intensity. A total of 20 classes are used (each class contains 77 days), with class # 1 being representative of the less strong SHL and class # 20 being representative of the most strong SHL in the 18-year period considered (1984–2001). Contours indicate the meridional gradient of the geopotential height (in mgp km^{-1}).

the low-level winds over West Africa. In particular, the south-westerly monsoon wind speed is governed by the surface pressure gradient between the high-pressure areas over the Atlantic Ocean and the low pressures associated with the SHL. From Figure 1, the decrease of 1000 hPa geopotential height in the SHL is concomitant to the increase of the meridional gradient of geopotential (between 10° and 20°N) just South of the lowest geopotential values (i.e. around 15°N).

5. Composite analysis of the West African monsoon circulation and convection patterns

The evolution of the regional-scale wind field and convection patterns as a function of the SHL intensity has been analysed through a composite analysis. In the following, we show only the results for the days with maximum and minimum SHL activity. The composite study was performed using classes # 1–3, for the days of weak SHL intensity and classes # 18–20, for the days of strong SHL intensity. Hence, each composite was computed on 231 days. This choice is made not only to select the extreme cases of SHL thickness but also to keep enough cases to perform a significant composite study. The inter-annual distribution of these extreme SHL cases is quite homogeneous (not shown). More cases of strong SHL events are found in August (0.17 of daily occurrence probability) than during the other months (0.14 in July and September and 0.15 in June). Note that the percentages are computed with respect to the total number of events detected during the summer over the 18 years period (1548 cases) and the duration of each month: June (10 days), July (31 days), August (31 days) and September (17 days). On the other hand, more weak SHL events are found in September (0.24 of daily occurrence probability) than during any other months (0.15 in July, 0.12 in August and 0.09 in June). Thus, September appears to be prone to weak SHL events.

6. Low-level monsoon circulation at the regional scale

The African monsoon winds at 925 hPa and the mean 925–700 hPa temperature are shown during days of weak SHL intensity (Figure 2(a)) and strong SHL intensity (Figure 2(b)). Higher mean temperatures in the 925–700 hPa layer are seen over a larger portion of West Africa during the period of strong SHL activity (Figure 2(b)) as opposed to the period of weak SHL activity (Figure 2(a)). This is coherent with the hypsometric equation, which links the average of the temperature in the layer and its thickness. The latitudinal location of the maximum temperature west of the Hoggar mountains (23°N, 5 °E) is nearly the same in both composites and is similar to that seen in climatology during the summer (e.g. LA09). During strong SHL episodes, the maximum of temperature is higher and located further west than during weak SHL events. The centre of the SHL is located at 5 °W and 2 °E during strong and weak SHL events, respectively. This could be associated with the west/east pulsation of the temperature field over Sahara identified by Chauvin *et al.* (2010).

As expected, the 925–700 hPa thickness influences the 925 hPa wind circulation at intra-seasonal time scale, especially the intensity of the cyclonic circulation around the depression centre. The increase of the thickness is accompanied by larger wind speeds, where the meridional and zonal gradient of the 925 hPa geopotential height is the strongest. We note also an increase of the northerly Harmattan winds to the west of the SHL and an increase of the monsoon flow south of the SHL, but only over the Sahel (i.e. between 10°N and 20°N).

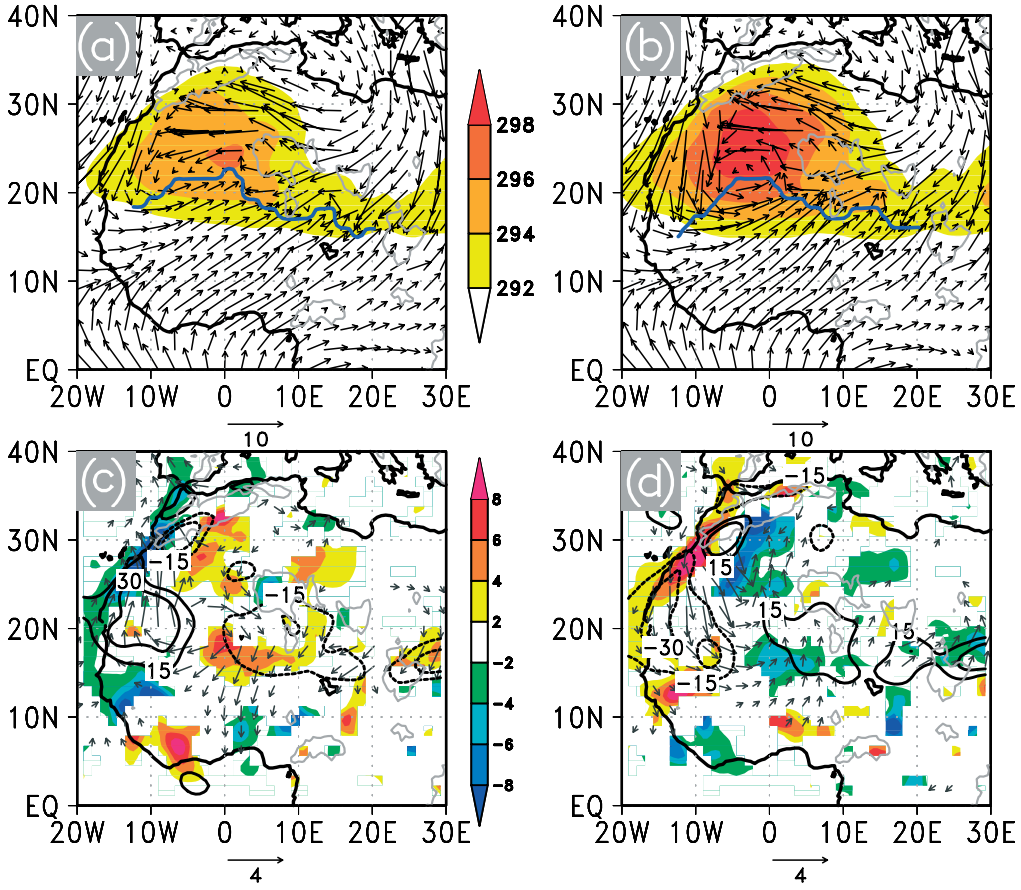

Figure 2. Mean 925 hPa wind field (in m s^{-1}, vectors) and temperature averaged between 700 and 925 hPa (in K, colour) for the weak SHL composite (a) and the strong SHL composite (b). The position of the ITD is given by the blue line. Anomaly of the 925–850 hPa integrated water vapour flux divergence (in g kg^{-1} day^{-1}, colour shaded), of the 700–850 hPa integrated moisture advection (in g kg^{-1} day^{-1}, black contour) and anomaly of 925 hPa wind (vectors, with significant larger than 90% using Student's *t*-test) during weak SHL (c) and strong SHL (d) phases with respect to the average of moisture advection and 925 hPa winds during the summer season.

The mean location of the ITD just south of the temperature maximum does not change significantly between the two composites (blue line in Figure 2). This is consistent with the fact that the fluctuations of intensity of the SHL do not influence its mean latitudinal position (Figure 1). However, the impact of the SHL intensity on the moisture advection is important. During strong SHL episodes, moistening (appearing as a positive anomaly with respect to the climatological mean over the summer period in contour Figure 2(d)) occurs over the Sahel, to the south-west of the Hoggar mountains. In contrast, drying (in the form of a dry anomaly) occurs along the Atlantic coast around 20°N (Figure 2(d)). The moistening over the central Sahel (east of 5 °W, i.e. over Mali and Niger) in this composite is related to the strengthening of the monsoon flow, bringing an excess of moisture from around 10°N and further north.

During weak SHL phases, drying is seen East of 5 °W (Figure 2(c)) associated with the decrease of the monsoon strength over the central Sahel. The anomaly of 925 hPa wind displays an anticyclonic circulation around the centre of the SHL (Figure 2(c)). This anomaly is associated with a moisture advection pattern opposite to that seen during strong SHL phases, with the moistening of the Sahel, west of 5 °W, i.e. over Senegal and surrounding countries.

In both weak and strong SHL, this area of moisture advection in the low troposphere is located very close to the ITD, where the horizontal moisture gradient is the strongest. This result is in accordance with the increase of the moisture flux south of the ITD (not shown). To the south of moistening areas, the integrated moisture flux divergence anomaly is negative (blue shading area), around 0 °E during strong SHL and around 10 °W during weak SHL, which could favour the upward advection of moisture and thus favour convective activity. In both weak and strong SHL, the anomalies of the low troposphere and the divergence of low-tropospheric moisture flux display a north–south dipole. Over the Sahel, this north–south dipole associated with a second east–west dipole, which could be linked with the 925 hPa wind field, produces a south–west to north–east tilt of the negative anomaly of the divergence anomaly during strong SHL (and positive anomaly during weak SHL) along the Saharan and Sahel area.

Note that the cyclonic circulation around the SHL was visible also in the 850 hPa wind field (not shown). However, during weak SHL events, the monsoon flow

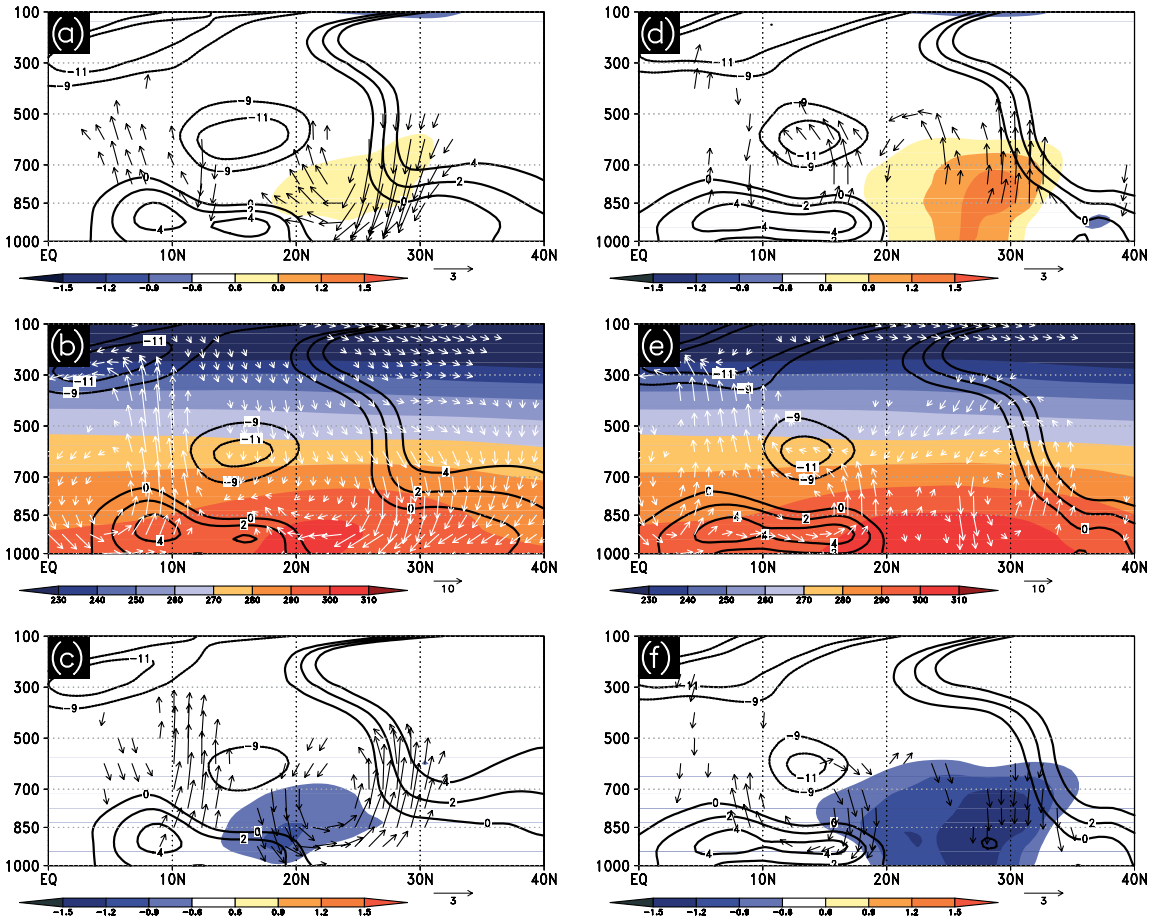

Figure 3. Mean vertical-latitudinal distribution, averaged between [20 °W; 5 °W] (left panels) and between [5 °W; 10 °E] (right panels), of the temperature anomaly (in K, colour), of the zonal wind (in m s^{-1}, black contours) and anomaly with respect to the mean summer circulation of meridional and vertical winds (in m s^{-1}) for the strong SHL composite (a and d) and the strong SHL composite (d and f). The significance of these results has been validated using Student's-*t* test. Only the significance of data larger than 90% are plotted. Summer mean climatology of temperature and wind fields for each boxes are added (b and e) using only 0600 UTC time step.

south of the SHL was much weaker and too shallow to reach that level. This level is very close to the altitude of the interface between the south-westerly monsoon layer and the overlaying north-easterly Saharan air layer (Parker *et al*., 2005). On the other hand, the monsoon flow could be detected during strong SHL events because it was deeper, its top being above 850 hPa. The deeper monsoon layer during stronger rather than weaker SHL events is shown in Figure 3.

In both strong and weak SHL phases, the moisture advection anomalies are essentially located over the Sahel. It is worth noting that there is no significant modulation of the moisture advection along the Gulf of Guinea between the composites. This could be due to the fact that during the summer, the moisture advection close to the Guinean coast is rather weak due to both weak winds and small horizontal gradient of moisture in this region.

7. Vertical structure of West African monsoon circulation

As discussed in the previous section, the low-level circulations and moisture advection over the Sahel exhibit distinct patterns on either side of a north–south oriented axis passing through the SHL at 5 °W. Hence, the vertical structure of the monsoon circulation during weak and strong SHL episodes has been decomposed along two latitudinal transects: a western transect along which variables are averaged between 20 °W and 5 °W (Figure 3(a) and (b)) and an eastern transect along which variables are averaged between 5 °W and 10 °E (Figure 3(c) and (d)).

Because of the method used, the largest temperature anomaly fields are located in the low troposphere (between 700 and 925 hPa). Furthermore, because the eastern transect captures a larger part of the SHL than the western one, larger low-level temperature anomalies are seen along the eastern transect.

The monsoon flow extends further north along the eastern transect, and it is stronger and deeper north of 10°N during strong SHL phases compared to weak SHL phases (as seen in the zonal component of the low-level winds). It appears that the location and the intensity of the African easterly jet (AEJ) are different, depending on whether we consider the eastern or the western transect. The characteristics of the jet also depend on the intensity of the SHL.

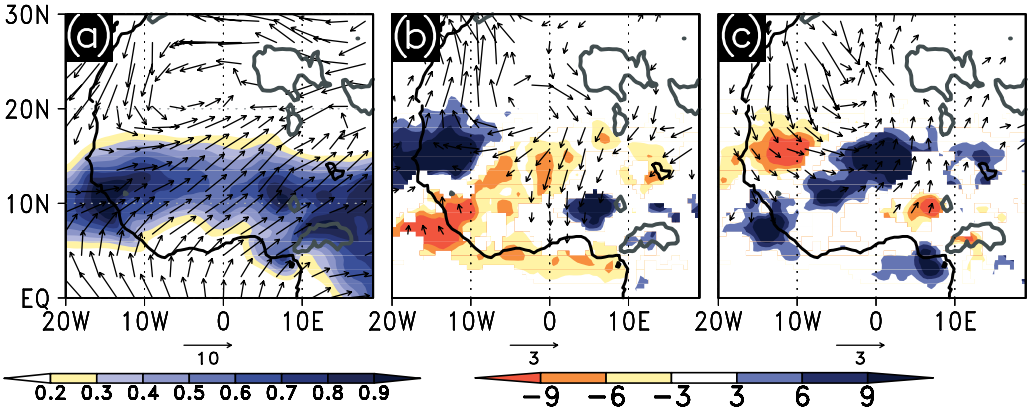

Figure 4. (a) Mean occurrence frequency of brightness temperature under 230 K (shaded) and mean 925 hPa wind circulation during the summer season (vectors, in m s^{-1}). Significant anomaly in relation to the summer average, of the convective activity (in %) based on the occurrence of brightness temperature under 230 K (see text for more details, colour), and anomaly, in relation to the mean summer circulation, of the wind field at 925 hPa (vectors, in m s^{-1}, significant at 90%) for the weak SHL composite (b) and the strong SHL composite (c), computed with respect to (a).

The largest difference is in the western box, when the maximum intensity of the AEJ occurs during the intense phases of the SHL and the minimum intensity occurs during the weak phases (Figure 3(a) and (c), respectively). The increase of the divergent circulation around 700 hPa associated with intense SHLs tends to increase the north-easterly return flow, which contributes to enhance the intensity of the AEJ.

As shown by Thorncroft and Blackburn (1999), an increase of the vertical velocity in the SHL can lead to an increase of the meridional gradient of temperature between the rainfall belt and the dry convection of the heat low. This tends to enhance the AEJ, with a maximum of 13 m s^{-1} in the strong SHL composite and 9 m s^{-1} in the weak SHL composite.

Along the eastern transect, significant ascending motions are seen to be co-located with the core of the SHL and just south of the ITD (between 15°N and 20°N) during the strong SHL phase (Figure 3(d)). These circulations looks like Figure 8 of Thorncroft and Blackburn (1999), where the authors illustrate the relationship between the meridional and the vertical circulation due to the SHL with the meridional circulation generated by the conservation of angular momentum.

Opposite wind circulations and temperature anomalies are observed during weak SHL activity (Figure 3(c)). Along the western transect, the largest ascent anomaly is observed during weak phases of the SHL (Figure 3(a)), and the deepest upward anomaly is visible around 13°N. The descending motions in the vicinity of the ITD are seen to be located directly over it (around 20°N) and slightly further north than along the eastern transect.

8. Convection

Anomalies of convection associated with the weak and strong phases of the SHL are now presented. These anomalies are performed with respect to the climatological mean occurrence frequency of convection during the summer (Figure 4(a)).

In the weak SHL composite, a significant positive anomaly of convection is evident west of about 10 °W and north of 12°N (Figure 4(b), with an increase larger than 10% of convective activity). This is found to be in agreement with the large increase of moisture advection anomaly shown in Figure 2(c) and the significant ascending motion visible to the north of 10°N along the western transect in Figure 3(a). To the south of 10°N, a negative anomaly of the convective activity is visible along the Atlantic coast, which is consistent with a northward migration of the convection band (shown in Figure 4(a)) to the west of the SHL.

Another region of significant positive anomaly of convection is seen just west of the Jos Plateau in Nigeria, consistent with the strong ascending motions in that region (Figure 3(c)), in spite of no significant modification of a moisture advection anomaly. Concomitant with the previously noted anomalous anticyclonic circulation around the SHL centre (Figure 2(c)), we see a decrease of the convective activity over the central and eastern part of the West African Sahel (Figure 4(b)).

Opposite convection patterns are associated with the strong SHL composite (Figure 4(c)), with an increase of the convective activity over the central Sahel, east of about 5 °W and along the Atlantic coast south of 10°N. The positive anomaly of convection over the central Sahel is positioned over a broad area of enhanced cyclonic circulation associated with an intensification of the monsoon flow. From 5 °W to 5 °E, a significant increase of the convective activity occurs between 10° and 17°N (+10% of convection). This result is in accordance with the increase of the upward wind observed south of the ITD, as shown in Figure 3(d), west of 10 °W, which suggests that the negative anomaly of convection seen over Senegal is related to both the southward migration of the convection band as shown in Figure 4(a) and the advection of dry air from the Sahara. A negative anomaly of convection is

also detected west of the Jos Plateau. Moreover, the area of the positive anomaly of convective activity is in accordance with the area of negative anomaly of the divergence flux (Figure 2(c) and (d)) during both extreme activities of the SHL.

It is worth noting that the widespread anomaly of enhanced convection associated with the strong SHL events exhibits a tilted, southwest–northeast-oriented structure, extending from Sierra Leone to Niger, and that this pattern of convection anomaly is roughly aligned with the mean direction of the low-level monsoon winds during the summer (see arrows in Figure 4(a)). Moreover, there is a strong similarity between the positive anomaly of convective activity from satellite data and the convergence of the moisture flux in the low levels (Figure 2(c) and (d)). This supports the impact of the inter-annual and spatial variability of the low troposphere moisture divergence flux on the convective activity over the Sahel. The relationship with the regions of positive moisture advection located to the north remains more complex. Flamant *et al.* (2007) have suggested a mechanism for cooling of the SHL by convection, due to the northward propagation of cold pools, reinforcing the monsoon flux and enhancing the advection of cold air masses over the desert.

To assess the duration and the temporal coherence of the SHL and convective anomalies, we have computed the temporal evolution of the SHL thickness anomaly over the Sahara (i.e. [10 °W;7 °E][20°N;30°N]) and of the convective activity anomaly averaged over the Sahel (i.e. between 10°N and 20°N) along both the western and eastern transects. Note that the significant convection anomalies detected over Sierra Leone and West of the Jos Plateau, located south of 10°N, are not accounted for. The temporal evolution of the composites is computed as follow:

(1) All extreme events of the SHL (maximum or minimum of intensity cases) are detected and given the time stamp 'D'.
(2) We then scan backward in time between $D-10$ and $D-1$, as well as forward in time between $D+1$ and $D+10$, to detect other extreme events (maximum or minimum of SHL intensity).
(3) Provided that an extreme event is detected between $D-10$ and $D-1$ (e.g. D_b), or $D+1$ and $D+10$ (e.g. D_f), only the time range between D_b+1 and D_f-1 (or D_b+1 and $D+10$ or $D-10$ and D_f-1) is taken into account in the final composite.

In our method, if two subsequent days are being classified as belonging to the period of maximum SHL intensity (i.e. belong to the classes # 18–20), then no data from the period $[D+1; D+10]$ will be included in the final composite (because D_f-1 is equal to D).

In Figure 5, the temporal evolution of the SHL in both strong or weak phases is plotted with respect to day D when the strongest or the weakest SHL is detected. The convection signal shown in Figure 4(b) and (c) reflects the state of the convection anomalies as they appear on Figure 5 on day D.

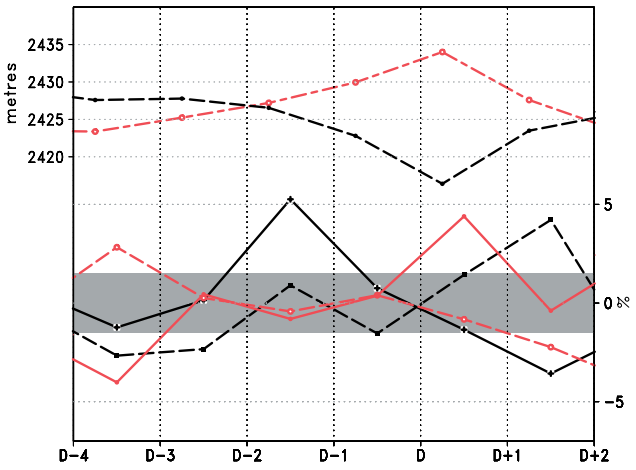

Figure 5. Temporal evolution of the SHL thickness averaged over the Sahara ([10 °W; 7 °E][19°N; 27°N], in m), between $D-4$ and $D+2$, with respect to day D that is the time when the SHL intensity is maximum (top red short–long-dashed line) or minimum (top black dashed line). Temporal evolution of the convective activity, defined by the anomaly of the number of grid box below 230 K with respect to the mean summer convective activity over the two boxes of the Sahel area [20 °W, 5 °W] (bottom dashed lines) and [5 °W, 10 °E] (bottom solid lines), during periods of strong SHL (red lines) or weak SHL (black lines). Grey shading area indicates the 90% level of significance.

The increase of the SHL depth is seen to be quite steady between $D-4$ and D during the strong SHL phase (red dashed line with closed circles) and to decrease more rapidly than it increased thereafter. Conversely, the decrease of the SHL depth during the weak SHL phase (black short–long dashed line with open circles) is very small between $D-4$ and $D-2$, while the SHL depth decreases more rapidly between $D-2$ and D.

During a strong SHL phase, the maximum of convective activity anomaly (+5%) in the eastern domain (i.e. between 5 °W and 10 °E) occurs on the same day (i.e. at D) as the maximum of SHL depth, while no significant convective activity anomalies are detected between $D-3$ and $D-1$ and on $D+1$. The decrease in convection anomaly between D and $D+1$ could be due to the characteristics of deep convection over West Africa (for instance the fact that the MCS propagate westward, Mathon and Laurent, 2001) and/or to the fact that deep convection this far north on day D day was likely detrimental to the SHL and led to its weakening (fast decrease of the SHL thickness between D and $D+1$ in Figure 5). One mechanism for the cooling of the SHL by convection is related to the northward propagation of cold pools associated with meso-scale convective systems, reinforcing the monsoon flux and enhancing the advection of cold air masses over the desert as shown by Flamant *et al.* (2007) and Flamant *et al.* (2009). The cooling in the region of the SHL leads to the weakening of the SHL and, in turn, is responsible for conditions that

are no longer favourable to the development of deep convection over the Sahel.

In the Western domain, no significant convection anomalies are detected between $D-3$ and $D-1$, while an increasing negative anomaly of convection is seen from D onward. This analysis also suggests that negative anomalies of convection may be slightly more persistent than positive anomalies of convection during this phase.

During the weak SHL phase, in the eastern domain, a maximum of convection is detected at $D-2$. The existence of deep convection over the Sahel, which is related to westward propagating meso-scale convective systems, is likely to have accelerated the weakening of the SHL as previously noted (i.e. an increase of the rate at which the SHL depth diminished was evident after $D-2$). The mechanism involved here is likely the cooling and moistening associated with the propagation of cold pools of meso-scale convective systems in the vicinity of the ITD (Flamant *et al*., 2007; Flamant *et al*., 2009).

Then, as the SHL collapses, conditions become detrimental to deep convection of the central and east Sahel as evident from the decrease in convection anomaly from a weak positive value on $D-1$ to large negative values on D and $D+1$. In the Western domain, the maximum of convection anomaly occurs at $D+1$, i.e. one day after the weakest SHL is detected. Part of the maximum convective activity detected here can be explained by the westward movement of the large-scale positive anomaly of convective anomaly detected two days later in the eastern part of the domain. This convective activity intensifies close to the coast where favourable conditions for convection are observed, such as the decrease of the Harmattan wind and the southerly wind anomaly south of the ITD associated with low SHL and of the presence of the coast. Prior to D, convection anomalies in this domain are mostly negative, except on $D-2$ when a weak positive convective anomaly is detected.

9. Summary and conclusions

To the best of the authors' knowledge, this study presents the first investigation of the regional-scale patterns of low-level atmospheric circulations and convection associated with weak and strong phases of the SHL during the summer, using 18 years of independent numerical-weather-prediction-model reanalysis data and satellite observations. Only intraseasonal fluctuations of the SHL under 60 days are used to build the classification of the SHL intensity during the summer period (20 June–17 September), while the SHL is located over the western Sahara. The regional-scale wind field and convection patterns are analysed using a composite analysis based on the SHL intensity.

In terms of latitude, the position of the centre of the SHL was found not to change as a function of SHL intensity and to remain around 22°N. This stationary location of the SHL could be related to the near constant location of the maximum summertime subsolar heating point and maximum surface temperature, as shown in LA09. In terms of longitude, the centre of the SHL during strong SHL episodes was detected further west than during weak SHL events (the centre is located at 5 °W and 2 °E during strong and weak SHL, respectively). These longitude displacements could be associated with the west/east pulsation of the temperature field over the Sahara identified by Chauvin *et al*. (2010).

Strong SHL phases are associated with (1) a positive low-level temperature anomaly; (2) a strengthening of the monsoon flow, a negative anomaly of the divergence flux around 15°N and an enhancement of the moisture advection from 10°N over the central Sahel (i.e. East of 5 °W); (3) an intensification of the AEJ and (4) an anomaly of upward vertical motion located south of the ITD, below the AEJ. These conditions appear to be favourable either to the occurrence of convection or to result from convective activity over the central Sahel (between 5 °W and 5 °E and between 10° and 17°N). An analysis of the temporal coherence between the SHL and convective anomalies shows that the strongest, most widespread convective activity over the central Sahel occurs on the day when the SHL intensity is strongest. Conversely, west of 5 °W, the strengthening of the north-easterly flow associated with the SHL circulation is accompanied by a southward movement of the main rainfall belt, an increase in dry advection from the Sahara and a significant decrease in the convective activity over Senegal. A negative anomaly of convection is also detected to the west of the Jos Plateau.

Opposite patterns are found during weak SHL phases with a negative anomaly of convection over the central Sahel connected with anomalous subsidence south of the ITD and drying (i.e. negative moisture advection) associated with a marked anomalous anticyclonic circulation at 925 hPa, preventing the monsoon flow from penetrating too far north over the continent. The lack of widespread convective activity over the central Sahel starts on the day when the SHL intensity is the weakest (more than 80% significance) and is minimum the following day. In contrast, convective activity is seen to increase west of 5 °W over Senegal and adjacent countries due to the weakening of the north-easterly flow associated with the SHL circulation along the Atlantic coast, which is responsible for a northward migration of the main rainfall belt and increased moisture advection and negative divergence flux inland. The strongest convective activity over Senegal occurs on the day following the SHL intensity minimum. The origin of this increase could be the westward propagation of the positive anomaly of convective activity observed two days later in the eastern Sahel. This anomaly of convection increases when it reaches the Senegal coast, which is why we do not observe its

propagation, as shown in in Figure 5. This increase could be due to the favourable conditions such as the closeness of the ocean, the decrease of the Harmattan wind and the increase of the monsoon wind. Grams *et al*. (2009) have observed and modelled the Atlantic inflow to the continent at 18°N. These penetrations of air masses during the night generate cooling and an increase of specific humidity between 16 °W and 11 °W. This moisture advection could favour the development of MCS during the daytime. Are these penetrations larger during periods where the Harmattan wind is less intense, thus during weak SHL events? In Figure 4(b), we note an increase of the convective activity over an area close to the domain studied by Grams *et al*. (2009). The relationship between the intensity or the location of the SHL and the penetrations of this cold and humid air is still open to interpretation.

It appears that the intra-seasonal pulsations of the SHL have a significant impact on the dynamics of the West African monsoon system during the summer season and are also likely to impact convection and rainfall over the Sahel. There is a robust, coherent correlation between the reinforcement of the cyclonic circulation over the Sahara during strong phases of the SHL and the increase of convective activity over the eastern Sahel. We have shown that the convective activity in the two boxes of the Sahel exhibits opposite trends following positive and negative extreme events of the SHL pulsations. Furthermore, this study suggests that there might be some predictability signal for deep convection (and possibly rainfall) associated with the state of the SHL and these key features, such as the intra-seasonal pulsation of the SHL, need to be well represented in seasonal forecast models.

Acknowledgements

On the basis of a French initiative, AMMA was built by an international scientific group and is currently funded by a large number of agencies, especially from France, the United Kingdom, the United States and Africa. It has been the beneficiary of a major financial contribution from the European Community's Sixth Framework Research Programme. Detailed information on scientific coordination and funding is available on the AMMA International web site http://www.amma-international.org.

References

Brest CL, Rossow WB, Roitier MD. 1997. Update the radiance calibration for ISCCP. *Journal of Atmospheric and Oceanic Technology* **14**: DOI: 10.1175/1520–0426.

Buckle C. 1996. *Weather and Climate in Africa*. Addison-Wesley Longman: Harlow.

Chauvin F, Roehrig R, Lafore J-P. 2010. Intraseasonal variability of the Saharan heat low and its link with mid-latitudes. *Journal of Climate* **23**: 2544–2561.

Couvreux F, Guichard F, Bock O, Campistron B, Lafore J-P, Redelseperger J-L. 2009. Synoptic variability of the monsoon flux over West Africa prior to the onset. *Quarterly Journal of the Royal Meteorological Society* AMMA Special Issue **136**: 159–173.

Flamant C, Chaboureau J-P, Parker DJ, Taylor C, Cammas J-P, Bock O, Timouk F, Pelon J. 2007. Airborne observations of the impact of a convective system on the planetary boundary layer thermodynamics and aerosols distribution in the inter-tropical discontinuity region of the West African monsoon. *Quarterly Journal of the Royal Meteorological Society* **133**: 1175–1189.

Flamant C, Knippertz P, Parker DJ, Chaboureau J-P, Lavaysse C, Agusti-Panareda A, Kergoat L. 2009. The impact of a meso-scale convective system cold pool on the northward propagation of the intertropical discontinuity over West Africa. *Quarterly Journal of the Royal Meteorological Society* **135**: 139–159.

Fu R, Del Genio A, Rossow WB. 1990. Behavior of deep convective clouds in the tropical Pacific from ISCCP radiances. *Journal of Climate* **3**: 1129–1152.

Grams CM, Jones SC, Marsham JM, Parker DJ, Haywood JM, Heuveline V. 2009. The Atlantic inflow to the Saharan heat low: Observations and modelling. *Quarterly Journal of the Royal Meteorological Society* **136**: 125–140. DOI: 10.1002/qj.429.

Kallberg P, Berrisford P, Hoskins B, Simmons A, Uppala S, Lamy-Thepaut S, Hine R. 2005. ERA-40 Atlas. Technical report ERA-40, Project Report Series, ECMWF: Shinfield Park, Reading; 1–191.

Knippertz P. 2008. Dust mobilization in the West African heat trough – the role of the diurnal cycle and of extratropical synoptic disturbances. *Meteorologische Zeitschrift* **17**(5): 553–563.

Lafore J-P, Chapelet P, Mumba Z, Chapelon N, Dufresne M-C, Agbabu R, Abdoul-Aziz A, Hamidou H, Asencio N, Couvreux F, Nuret M, Garba A. 2007. Forecaster's Guide for West African Synthetic Analysis/Forecast. https://www.amma-eu.org/workspaces/work_package_s_workspace/process-studies/wp2_1/deliverables/forecaster-s-guide-for.

Lavaysse C, Flamant C, Janicot S, Knippertz P. 2010. Links between African easterly waves, midlatitude circulation and intraseasonal pulsations of the West African heat low. *Quarterly Journal of the Royal Meteorological Society* **136**: 141–158.

Lavaysse C, Flamant C, Janicot S, Parker DJ, Lafore J-P, Sultan B. 2009. Seasonal evolution of the West African heat low, a climatological perspective. *Climate Dynamics* **33**: 313–330. DOI: 10.1007/s00382-009-0553-4.

Lenters JD, Cook KH. 1995. Simulation and diagnosis of the regional summertime precipitation climatology of South America. *Journal of Climate* **8**: 2988–3005.

Mathon V, Laurent H. 2001. Life cycle of Sahelian mesoscale convective cloud systems. *Quarterly Journal of the Royal Meteorological Society* **127**: 377–406.

Parker DJ, Thorncroft CD, Burton R, Diongue-Niang A. 2005. Analysis of the African easterly jet, using aircraft observations from the JET 2000 experiment. *Quarterly Journal of the Royal Meteorological Society* **131**: 1461–1482.

Ràcz Z, Smith RK. 1999. The dynamics of the heat low. *Quarterly Journal of the Royal Meteorological Society* **125**: 225–252.

Redelsperger JL, Thorncroft CD, Diedhiou A, Lebel T, Parker DJ, Polcher J. 2006. African monsoon multidisciplinary analysis: an international research project and field campaign. *Bulletin of the American Meteorological Society* **87**: 1739–1746.

Spengler T, Smith RK. 2008. The dynamics of heat lows over flat terrain. *Quarterly Journal of the Royal Meteorological Society* **134**: 2157–2172.

Sultan B, Janicot S, Diedhiou A. 2003. The West African Monsoon dynamics. part I: documentation of intraseasonal variability. *Journal of Climate* **16**(21): 3389–3406.

Thorncroft CD, Blackburn M. 1999. Maintenance of the African easterly jet. *Quarterly Journal of the Royal Meteorological Society* **125**(555): 763–786.

Torrence C, Compo GP. 1998. A practical guide to Wavelet analysis. *Bulletin of the American Meteorological Society* **79**: 61–78.

